PPPL-2116

UC20-F

PPPL-2116

HARMONIC GENERATION AND PARAMETRIC DECAY IN THE ION CYCLOTRON FREQUENCY RANGE

By

F.N. Skiff, K.L. Wong, and M. Ono

JUNE 1984

PLASMA PHYSICS LABORATORY

PRINCETON UNIVERSITY
PRINCETON, NEW JERSEY

PREPARED FOR THE U.S. DEPARTMENT OF ENERGY,
UNDER CONTRACT DE-AC02-76-CHO-3073.

NOTICE

Printed in the United States of America.

Available from:

National Technical Information Service
U. S. Department of Commerce
5285 Port Royal Road
Springfield, Virginia 22151

Price: Printed Copy $__*__; Microfische $3.50

*PAGES	NTIS Selling Price
1-25	$5.00
26-50	$6.50
51-75	$8.00
76-100	$9.50
101-125	$11.00
126-150	$12.50
151-175	$14.00
176-200	$15.50
201-225	$17.00
226-250	$18.50
251-275	$20.00
276-300	$21.50
301-325	$23.00
326-350	$24.50
351-375	$26.00
376-400	$27.50
401-425	$29.00
426-450	$30.50
451-475	$32.00
476-500	$33.50
500-525	$35.00
526-550	$36.50
551-575	$38.00
576-600	$39.50

For documents over 600 pages, add $1.50 for each additional 25 page increment.

HARMONIC GENERATION AND PARAMETRIC DECAY IN THE ION CYCLOTRON FREQUENCY RANGE

PPPL--2116
DE84 015147

F. N. Skiff, K. L. Wong, and M. Ono
Plasma Physics Laboratory, Princeton University
Princeton, New Jersey 08544

ABSTRACT

Harmonic generation and parametric decay are examined in a toroidal ACT-I plasma using electrostatic plate antennas. The harmonic generation, which is consistent with sheath rectification, is sufficiently strong that the nonlinearly generated harmonic modes themselves decay parametrically. Resonant and nonresonant parametric decay of the second harmonic are observed and compared with uniform pump theory. Resonant decay of lower hybrid waves into lower hybrid waves and slow ion cyclotron waves is seen for the first time. Surprisingly, the decay processes are nonlinearly saturated, indicating absolute instability.

The successful application of high power rf heating schemes generally requires an understanding of nonlinear mechanisms which come into play in plasmas subjected to strong electric fields. Fortunately many nonlinear processes can be studied on small-scale devices where measurements are more easily performed. In this letter we report observations of harmonic generation and subsequent parametric decay of the second harmonic at low power levels in the low density toroidal ACT-1 plasma using electrostatic plate antennas. Resonant decay of lower hybrid waves into lower hybrid waves and slow ion cyclotron (electron-ion Buchsbaum) waves is seen for the first time.

The harmonic generation is consistent with plasma sheath rectification at the antenna, and uniform pump theory provides accurate predictions of the unstable frequencies for parametric decay. The saturated amplitude of the decay, however, does not scale exponentially with the pump power, but linearly, even at pump levels close to threshold. This scaling indicates a nonlinear saturation mechanism rather than convective saturation of the decay.

The plasma used in this experiment was produced in the ACT-I device using a biased hot filament source in the toroidal magnetic field which is adjustable up to 4.2 kG. Plasma temperatures of $T_e \approx T_i \approx 1$ eV, density $n \approx 0.5\text{-}1 \times 10^{10}$, and low collisionality $\nu_i/\Omega_{ci} \approx 10^{-3}$ were typical. Two curved metal plates, separated toroidally by 1 port (16.7 cm) and driven in antiphase through a matching network, served as an antenna. The driver frequency ω_D was chosen between $1\text{-}2 \times \Omega_{ci}$ which, for the slow wave and $\omega_{pi} \approx 2 \times \Omega_{ci}$, corresponds to a second harmonic ion Bernstein wave. For the harmonics, however, $n \times \omega_D > \omega_{LH} = (\omega_{pi}{}^2 + \Omega_{ci}{}^2)^{1/2}$ so that these frequencies correspond to lower hybrid waves. Edge regions of laboratory plasmas are in this regime. A schematic of the experimental setup is shown in Fig. 1(a).

To model the coupling of an electrostatic antenna one may start with the equation for the potential Φ

$$\nabla \cdot \overleftrightarrow{\varepsilon} \cdot \nabla \Phi = 4\pi \rho_{free},$$

where $\overleftrightarrow{\varepsilon}$ is the hot uniform-plasma dielectric tensor.[2] ρ_{free} refers to electric space charge not included in the uniform plasma model, in particular, to the charge on the antenna conductors and on the surface of the plasma sheath. Because of the behavior of the sheath, both the displacement and conduction currents from the antenna have a nonlinear component, the former due to nonlinear sheath capacitance[3] and the latter to sheath rectification.[4] Because sheath rectification is dominant, the current-voltage characteristic of the antenna can be estimated by

$$\imath = \frac{n_o v_t A}{4} \times e^{\frac{eV_a}{kT_e}},$$

where $\imath$ is the antenna current, n_o is the density in the sheath, v_t is the electron thermal velocity corresponding to the electron temperature T_e, and A is the effective plate area. (An accurate determination of A requires consideration of the effect of the magnetic field.) With antenna voltage $V_a = V_o \times e^{\imath\omega t}$ the amplitude of the n^{th} harmonic in the current is

$$\frac{i_n}{i_o} = I_{n-1}\left(\frac{eV_o}{kT_e}\right)/I_o\left(\frac{eV_o}{kT_e}\right) .$$

I_m denotes the modified Bessel function of order m. Figure 1(b) shows the observed harmonic amplitude ratios A_2/A_1, A_3/A_1, and A_4/A_1 (A_1 being the driver amplitude, etc.) as a function of eV_a/kT_e, the ratio of antenna voltage to plasma electron temperature. Shown for comparison are theor tical values of the above ratios, based on sheath rectification and evaluating the single parameter, eV_a/kT_e, for 1 W of antenna power. Observation of the resonance cones of the harmonics using radial scanning rf probes confirm that the harmonics are being generated near the antenna. It is also evident from the presence of resonance cones and the magnitude of the cone angles, given by

$$\tan^2\Theta = \frac{\omega_{pe}^2}{\omega^2} \times \left(\frac{\omega^2-\Omega_{ci}^2}{\omega^2-\omega_{LH}^2}\right)$$

that the harmonics are propagating as lower hybrid waves.

As the density is increased, the amount of harmonic generation decreases. Simultaneous changes in the linear loading make the density effect hard to quantify, but it is consistent with our simple model which predicts that at constant antenna power the sheath will exhibit less nonlinearity at higher densities. In principal, the nonlinearity can also be reduced by increasing T_e and/or by reducing A.

While harmonic generation is confined to the sheath region, the spectrum is additionally enriched by nonlinear wave-wave and wave-particle interactions in the plasma bulk. In particular, in this experiment we observed both resonant and nonresonant parametric decay of the second harmonic. The growth rate for these decays is given by

$$\gamma = \frac{-\mathrm{Im}(\varepsilon) + \Sigma_{\sigma,\eta} \frac{1}{8} |\vec{\mu}_\sigma - \vec{\mu}_\eta| \, \mathrm{Im}\left(\frac{\chi_\sigma \chi_\eta}{\varepsilon}\right)_\omega}{|\partial\varepsilon/\partial\omega_-|} , \qquad (1)$$

with $$\mu_\sigma = \left(\frac{q}{m}\right)_\sigma \left[\left(\frac{E_{0\parallel} k_\parallel}{\omega_0^2} + \frac{\vec{E}_{0\perp} \cdot \vec{k}_\perp}{\omega_0^2 - \Omega_\sigma^2}\right)^2 + \frac{|\vec{E}_{0\perp} \times \vec{k}_\perp|^2 \, \Omega_\sigma^2}{(\omega_0^2 - \Omega_\sigma^2)^2 \, \omega_0^2}\right]^{1/2} .$$

$\varepsilon = 1 + \chi_e + \chi_i = \hat{k} \cdot \overleftrightarrow{\varepsilon} \cdot \hat{k}$ is the scalar projection of the dielectric tensor, ω_0, ω_-, ω are the angular frequencies of the pump, lower sideband and low frequency wave or quasimode, respectively, and Ω_σ is the cyclotron frequency of species σ.

Two distinct decay processes were observed involving the second harmonic as pump. Figure 2(a) shows the complete spectrum including driver (F_0), second harmonic ($2F_0$), upper and lower sidebands (USB_1, USB_2, LSB_1, LSB_2), and corresponding low frequency excitations (QM_1, LF_2). One process (subscript 1) is the well-known decay of a lower hybrid wave into a lower hybrid wave and an ion cyclotron quasimode.[7] The other process (2) (not seen previously) is the resonant decay of a lower hybrid wave into a lower hybrid wave and an ion cyclotron wave (sometimes called a Buchsbaum mode)[8] with $\omega < \Omega_{ci}$ and

$$\frac{k_\perp}{k_\parallel} = \frac{\omega_{pe}}{\omega} \times \left(\frac{\omega^2 - \Omega_{ci}^2}{\omega^2 - \omega_{LH}^2}\right)^{1/2} .$$

The two decay processes can be readily distinguished by the frequencies of the decay waves. Data plotted in Fig. 2(b) pertain to both decays as observed over a range of toroidal field strengths. Observed decay wave frequencies are compared with the frequencies determined by Eq. (1) to be the most unstable. It is found that the quasimode frequency is always close to f_{ci} and that the frequency of the ion cyclotron wave is strongly constrained by the matching condition $k_0 = k_- + k$.

Observation of the decay wave amplitudes also provides information concerning the nature of the decay process. Resonant decays are constrained by the Manley-Rowe relations $N_0 + N_- =$ const. and $N_0 + N =$ const. where N_0 refers to the wave "action" of the pump (etc.).[9] Wave amplitude is proportional to wave action. In Fig. 2(c) the ratios A_{LSB2}/A_{LF2}, A_{LSB1}/A_{QM1}, $A_{LSB2}/A_{2F\phi}$, and $A_{LSB1}/A_{2F\phi}$ are plotted as functions of the squared amplitude of the second harmonic. For the resonant decay (subscript 2), the ratio of the decay wave amplitudes is a constant, in agreement with Manley-Rowe, since $N_-=N=0$ and $N_0=N_0^i$ at t=o gives for t>o

$$A_{LF}/A_{LSB} \propto \frac{N}{N_-} = \frac{(N_0^i-N_0)}{(N_0^i-N_0)} = 1$$

For the nonresonant decay this scaling does not hold and the decay wave amplitudes are determined by the decay saturation mechanism.[10] Above threshold the observed sideband amplitudes are proportional to the pump amplitude $A_{2F\phi}$ [Fig. 2(c)] indicating nonlinear saturation for both decay types. This behavior is surprising in view of the fact that parametric decay of lower hybrid waves is expected to be convective.[11] The same amplitude scaling has, however, been seen on an earlier experiment.[11] One possible explanation is that the decay is made absolute by reflective trapping of the decay waves. (In contrast to the earlier experiments, ACT-1 has no ends.) The finite spatial extent of the pump can accomplish reflective trapping through the effect of the pump on the decay wave wave numbers.[12,13] Treating the pump as a square potential "well," a rough estimate of the threshold for absolute instability is:

$$|r_1 r_2 e^{\Gamma L}| > 1 \ ,$$

where r_1 and r_2 are the (unequal) well wall reflectivities, Γ is the spatial growth rate $\Gamma = \gamma/v_{group}$, and L is the pump cone width as transited by the decay wave. For absolute instability the group velocities of the decay waves must be oppositely directed. The threshold condition reduces for our experiment to:

$$r_1 r_2 e^{\Gamma L} \sim \frac{\gamma^2}{8\omega\omega_-} e^{2\pi \ \gamma/\omega} > 1.$$

This threshold is very close to the convective threshold and very similar in scaling. For lower hybrid waves at higher frequency it is interesting to note that one of the reflections (nearly tangent) becomes strong and the other weak thereby reducing the convective threshold by a factor of two. Experimentally it is often the case (when there are resonance cones) that the observed thresholds are lower than convective estimates.[11] Further work is required to resolve this issue.

In summary, we have observed substantial harmonic generation associated with the use of an electrostatic antenna in the ion cyclotron frequency range. These harmonics have sufficient intensity to decay parametrically through both resonant and nonresonant channels. The decay wave amplitude scaling indicates absolute rather than convective instability.

ACKNOWLEDGMENTS

We thank G. A. Wurden for first noticing the spectrum, Liu Chen for helpful discussions, and J. Taylor and W. Kineyko for their technical assistance.

This work has been supported by the U.S. Department of Energy Contract No. DE-AC02-76-CHO-3073.

F. Skiff is supported by a Fannie and John Hertz Foundation Fellowship.

REFERENCES

1 M. Ono, K. L. Wong, and G. A. Wurden, Phys. Fluids 26, 298 (1983).

2 T. H. Stix, Theory of Plasma Waves (McGraw Hill, New York, 1962).

3 A. J. Cohen and G. Bekefi, Phys. Fluids 14, 1512 (1971).

4 S. J. Crawford and R. F. Meodnosky, J. Geophys. Res. 69, 2765 (1964).

5 J. L. Hirshfield and I. B. Bernstein, Phys. Fluids 18, 1787 (1975).

6 Khorasanov et al., Sov. Tech. Phys. Lett. 3(11), 470 (1977).

7 K. L. Wong and M. Ono, Phys. Rev. Lett. 47, 842 (1981).

8 S. J. Buchsbaum, Phys. Fluids 3, 418 (1960).

9 A. A. Galeev and R. S. Sagdeev, "Nonlinear Plasma Theory" in Reviews of Plasma Physics, 7 (Plenum, New York, 1979) 16.

10 K. Nishikawa and C. S. Liu, in Advances in Plasma Physics, Vol. 6, (John Wiley, New York, 1976) 67.

11 K. L. Wong, J. R. Wilson, and M. Porkolab, Phys. Fluids 23, 96 (1980).

12 D. F. Dubois, D. W. Forslund, and E. A. Williams, Phys. Rev. Lett. 33, 1013 (1974).

13 G. Picard and T. W. Johnston, Phys. Rev. Lett. 51, 574 (1983).

FIGURE CAPTIONS

1. Observations of Harmonic Generation

   (a) Experimental setup on ACT-I with electrostatic launchers.

   (b) Solid line harmonic ratios from sheath rectification. Points are amplitudes from the spectrum analyzer.

2. Observations of Parametric Decay

   (a) Parametric decay spectrum showing driver pump (second harmonic), and resonant(2) and nonresonant(1) decay products.

   (b) Decay product frequencies as a function of magnetic field intensity. Square points are calculated from uniform pump theory. Solid curves are based on data (x marks).

   (c) Decay product amplitude ratios vs antenna power.

#84X0270

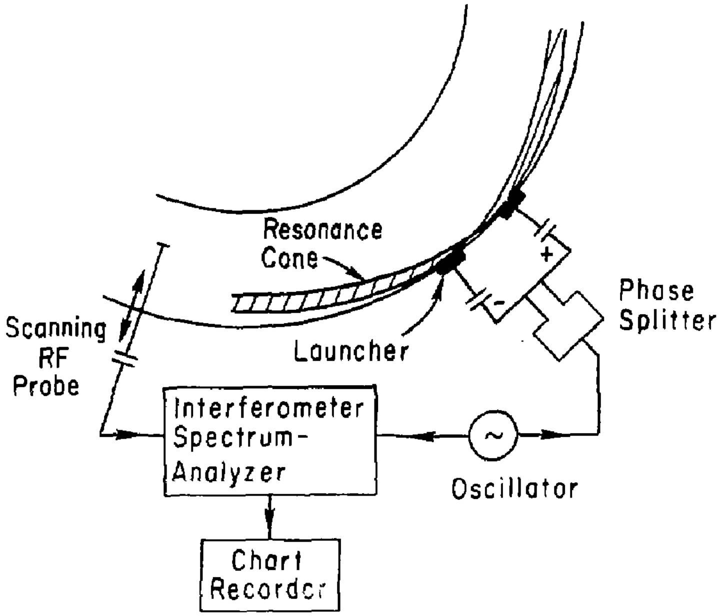

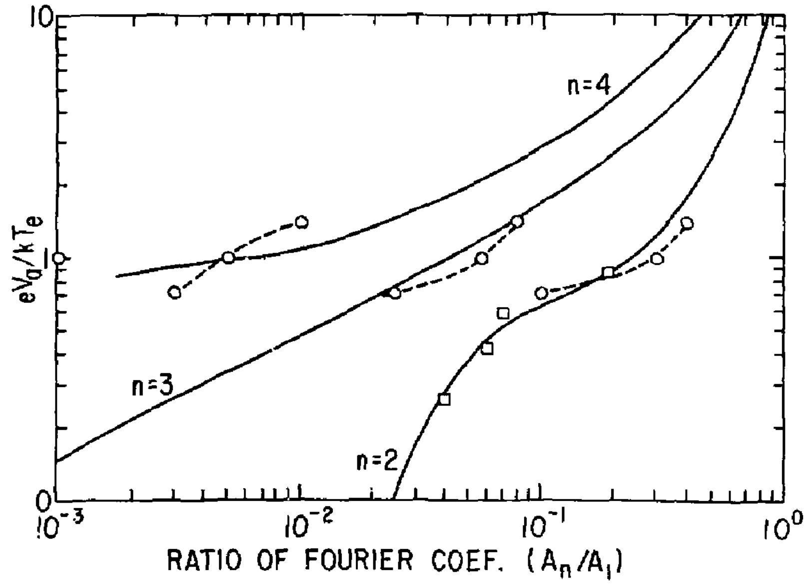

Fig. 1

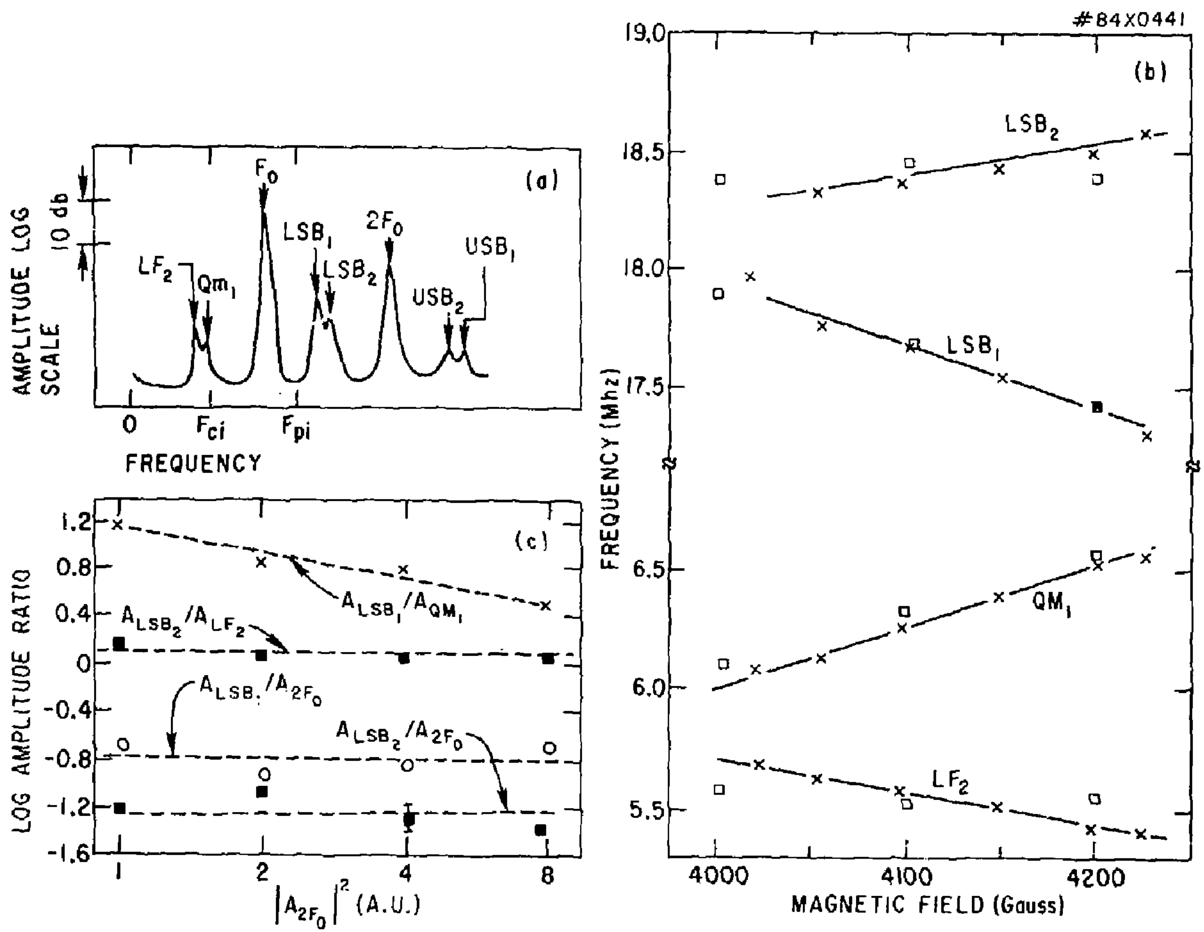
#84X0441
(a)
AMPLITUDE LOG SCALE
10 db
F0
LF2
Qm1
LSB1
LSB2
2F0
USB2
USB1
0
Fci
Fpi
FREQUENCY
(c)
LOG AMPLITUDE RATIO
ALSB1/AQM1
ALSB2/ALF2
ALSB1/A2F0
ALSB2/A2F0
|A2F0|2 (A.U.)
(b)
LSB2
LSB1
QM1
LF2
FREQUENCY (Mhz)
MAGNETIC FIELD (Gauss)

Fig. 2

EXTERNAL DISTRIBUTION IN ADDITION TO TIC UC-20

Plasma Res Lab, Austra Nat'l Univ, AUSTRALIA
Dr. Frank J. Paoloni, Univ of Wollongong, AUSTRALIA
Prof. I.R. Jones, Flinders Univ., AUSTRALIA
Prof. M.H. Brennan, Univ Sydney, AUSTRALIA
Prof. F. Cap, Inst Theo Phys, AUSTRIA
Prof. Frank Verheest, Inst theoretische, BELGIUM
Dr. D. Palumbo, Dg XII Fusion Prog, BELGIUM
Ecole Royale Militaire, Lab de Phys Plasmas, BELGIUM
Dr. P.H. Sakanaka, Univ Estadual, BRAZIL
Dr. C.R. James, Univ of Alberta, CANADA
Prof. J. Teichmann, Univ of Montreal, CANADA
Dr. H.M. Skarsgard, Univ of Saskatchewan, CANADA
Prof. S.R. Sreenivasan, University of Calgary, CANADA
Prof. Tudor W. Johnston, INRS-Energie, CANADA
Dr. Hannes Barnard, Univ British Columbia, CANADA
Dr. M.P. Bachynski, MPB Technologies, Inc., CANADA
Zhengwu Li, SW Inst Physics, CHINA
Library, Tsing Hua University, CHINA
Librarian, Institute of Physics, CHINA
Inst Plasma Phys, Academia Sinica, CHINA
Dr. Peter Lukac, Komenskeho Univ, CZECHOSLOVAKIA
The Librarian, Culham Laboratory, ENGLAND
Prof. Schatzman, Observatoire de Nice, FRANCE
J. Radet, CEN-BP6, FRANCE
AM Dupas Library, AM Dupas Library, FRANCE
Dr. Tom Mual, Academy Bibliographic, HONG KONG
Preprint Library, Cent Res Inst Phys, HUNGARY
Dr. S.K. Trehan, Panjab University, INDIA
Dr. Indra, Mohan Lal Das, Banaras Hindu Univ, INDIA
Dr. L.K. Chavda, South Gujarat Univ, INDIA
Dr. R.K. Chhajlani, Var Ruchi Marg, INDIA
P. Kaw, Physical Research Lab, INDIA
Dr. Phillip Rosenau, Israel Inst Tech, ISRAEL
Prof. S. Cuperman, Tel Aviv University, ISRAEL
Prof. G. Rostagni, Univ Di Padova, ITALY
Librarian, Int'l Ctr Theo Phys, ITALY
Miss Clelia De Palo, Assoc EURATOM-CNEN, ITALY
Biblioteca, del CNR EURATOM, ITALY
Dr. H. Yamato, Toshiba Res & Dev, JAPAN
Prof. M. Yoshikawa, JAERI, Tokai Res Est, JAPAN
Prof. T. Uchida, University of Tokyo, JAPAN
Research Info Center, Nagoya University, JAPAN
Prof. Kyoji Nishikawa, Univ of Hiroshima, JAPAN
Prof. Sigeru Mori, JAERI, JAPAN
Library, Kyoto University, JAPAN
Prof. Ichiro Kawakami, Nihon Univ, JAPAN
Prof. Satoshi Itoh, Kyushu University, JAPAN
Tech Info Division, Korea Atomic Energy, KOREA
Dr. R. England, Civdad Universitaria, MEXICO
Bibliotheek, Fom-Inst Voor Plasma, NETHERLANDS
Prof. B.S. Liley, University of Waikato, NEW ZEALAND
Dr. Suresh C. Sharma, Univ of Calabar, NIGERIA
Prof. J.A.C. Cabral, Inst Superior Tech, PORTUGAL
Dr. Octavian Petrus, ALI CUZA University, ROMANIA
Prof. M.A. Hellberg, University of Natal, SO AFRICA
Dr. Johan de Villiers, Atomic Energy Bd, SO AFRICA
Fusion Div. Library, JEN, SPAIN
Prof. Hans Wilhelmson, Chalmers Univ Tech, SWEDEN
Dr. Lennart Stenflo, University of UMEA, SWEDEN
Library, Royal Inst Tech, SWEDEN
Dr. Erik T. Karlson, Uppsala Universitet, SWEDEN
Centre de Recherchesen, Ecole Polytech Fed, SWITZERLAND
Dr. W.L. Weise, Nat'l Bur Stand, USA
Dr. W.M. Stacey, Georg Inst Tech, USA
Dr. S.T. Wu, Univ Alabama, USA
Prof. Norman L. Oleson, Univ S Florida, USA
Dr. Benjamin Ma, Iowa State Univ, USA
Prof. Magne Kristiansen, Texas Tech Univ, USA
Dr. Raymond Askew, Auburn Univ, USA
Dr. V.T. Tolok, Kharkov Phys Tech Ins, USSR
Dr. D.D. Ryutov, Siberian Acad Sci, USSR
Dr. G.A. Eliseev, Kurchatov Institute, USSR
Dr. V.A. Glukhikh, Inst Electro-Physical, USSR
Institute Gen. Physics, USSR
Prof. T.J. Boyd, Univ College N Wales, WALES
Dr. K. Schindler, Ruhr Universitat, W. GERMANY
Nuclear Res Estab, Julich Ltd, W. GERMANY
Librarian, Max-Planck Institut, W. GERMANY
Dr. H.J. Kaeppler, University Stuttgart, W. GERMANY
Bibliothek, Inst Plasmaforschung, W. GERMANY